

Neural Belief Reasoner

Haifeng Qian

IBM T. J. Watson Research Center
Yorktown Heights, NY
qianhaifeng@us.ibm.com

Abstract

This paper proposes a new generative model called neural belief reasoner (NBR). It differs from previous models in that it specifies a belief function rather than a probability distribution. Its implementation consists of neural networks, fuzzy-set operations and belief-function operations, and query-answering, sample-generation and training algorithms are presented. This paper studies NBR in two tasks. The first is a synthetic unsupervised-learning task, which demonstrates NBR’s ability to perform multi-hop reasoning, reasoning with uncertainty and reasoning about conflicting information. The second is supervised learning: a robust MNIST classifier. Without any adversarial training, this classifier exceeds the state of the art in adversarial robustness as measured by the L_2 metric, and at the same time maintains 99% accuracy on natural images. A proof is presented that, as capacity increases, NBR classifiers can asymptotically approach the best possible robustness.

1 Introduction

It is a widely held hypothesis that bridging the gap between machine learning and reasoning would bring benefits to both domains. For reasoning systems, this could provide an elegant solution to automatically discover rules from observations, and could provide new approaches to reasoning with uncertainty. On the other hand, despite the phenomenal successes of deep learning, neural networks tend to have poor robustness and interpretability, both of which are non-issue in reasoning systems. The robustness issue has recently been highlighted by the existence of adversarial examples in many systems. For example, even for the well-studied MNIST task, the state of the art in L_2 robustness is far from satisfactory and comes at a cost of accuracy on natural images. More discussions are in Section 5.

There are numerous works at the intersection of machine learning and reasoning, some of which will be reviewed in Section 5. A prominent one is Boltzmann machine and its variants (Salakhutdinov and Hinton 2009), which combine neural networks and Markov random field that is a form of reasoning with uncertainty. A recent example is differentiable inductive logic programming (Evans and Grefenstette 2018), which combines neural networks and logic programs.

This paper presents a new approach called neural belief reasoner (NBR), which combines neural networks and belief functions. Belief function is a generalization of probability function (Shafer 1976), and has the advantage of modeling epistemic uncertainty, i.e., the lack of knowledge, and an elegant way of combining multiple sources of information. Despite these advantages, belief function has seen much less adoption than mainstream methods like Bayesian network and Markov random field. NBR is built on two innovations: 1) using neural networks to represent fuzzy sets, and 2) using fuzzy sets to specify a belief function. From the machine-learning perspective, NBR is a new generative model that specifies a belief function rather than a probability distribution. From the reasoning perspective, NBR is a new system of reasoning with uncertainty that enables automatic discovery of non-symbolic rules from observations and that uses belief functions to model uncertainty.

The next section will define the model and present query-answering, sample-generation and training algorithms. Then Sections 3 and 4 demonstrate NBR’s capabilities through two tasks. The first task is unsupervised learning: in a synthetic 11-bit world where only partial observations are available, an NBR model is trained and then answers queries. The queries involve calculating belief and plausibility of a proposition conditioned on another, and demonstrate multi-hop reasoning, reasoning with uncertainty and reasoning about conflicting information. The second task is supervised learning: a robust MNIST classifier. Techniques to adapt NBR for classification and techniques specific for robustness will be presented. The resulting classifier sets a new state of the art in adversarial robustness as measured by the L_2 metric, and at the same time maintains 99% accuracy on natural images. A proof is presented that, with more capacity, NBR classifiers can asymptotically approach the best possible robustness on the training set. This is the first such proof in literature.

2 Neural Belief Reasoner

Let’s start with a restricted framework of reasoning in Section 2.1, which serves as a stepping stone towards NBR’s definitions in Section 2.2 and algorithms after that.

2.1 Prototype with classical sets

Let U denote the sample space, i.e., the set of all possibilities. Consider a reasoning framework where a model is composed of K sets, $R_1, \dots, R_K \subseteq U$, and each R_i is annotated with a scalar $0 \leq b_i \leq 1$. Let's interpret each R_i as a logic rule: an outcome $x \in U$ is said to satisfy R_i if and only if $x \in R_i$. Let's interpret b_i as the belief in R_i .

Define vector $\mathbf{y} \triangleq (y_1, \dots, y_K)$ where entries are 0 or 1. Define intersection sets $S_{\mathbf{y}} \triangleq \bigcap_{1 \leq i \leq K | y_i=1} R_i$, and define $S_{(0, \dots, 0)} \triangleq U$. Intuitively each $S_{\mathbf{y}}$ contains outcomes that satisfy a subset of the K rules as selected by \mathbf{y} . Define scalar function $p(\mathbf{y}) \triangleq \prod_{i=1}^K (b_i \cdot y_i + (1 - b_i) \cdot (1 - y_i))$.

Let 2^U denote the power set of U . Define the following function from 2^U to \mathbb{R} : $m(\emptyset) \triangleq 0$; for $A \neq \emptyset$,

$$m(A) \triangleq \frac{\sum_{\mathbf{y} | S_{\mathbf{y}}=A} p(\mathbf{y})}{1 - \sum_{\mathbf{y} | S_{\mathbf{y}}=\emptyset} p(\mathbf{y})} \quad (1)$$

It is straightforward to verify that $\sum_{A \subseteq U} m(A) = 1$. Therefore this function $m(\cdot)$ satisfies the requirements to be a basic probability assignment (Shafer 1976). Hence this function $m(\cdot)$ uniquely specifies a belief function over U (Shafer 1976): $\text{Bel}(A) = \sum_{B \subseteq A} m(B)$, $\forall A \subseteq U$.

Intuitively this framework considers 2^K possible worlds: each world corresponds to each \mathbf{y} , and in each world a subset of the K rules, as selected by \mathbf{y} , exist. Each satisfiable world, i.e., where $S_{\mathbf{y}} \neq \emptyset$, is assigned a mass that is proportional to $p(\mathbf{y})$, the product of b_i 's for rules that are present and $(1 - b_i)$'s for rules that are absent. Each unsatisfiable world, i.e., where $S_{\mathbf{y}} = \emptyset$, is assigned a mass of zero. The total mass is one, which is achieved through the denominator in (1) that is essentially Dempster's rule of combination (Shafer 1976).

With a belief function defined, this framework is able to answer queries. Similar to conditional probabilities in traditional models, it answers with conditional belief functions. Given a condition $C \subseteq U$ and a proposition $Q \subseteq U$, the conditional belief and conditional plausibility are¹

$$\begin{aligned} \text{Bel}(Q | C) &= \frac{\text{Bel}(Q \cup \bar{C}) - \text{Bel}(\bar{C})}{1 - \text{Bel}(\bar{C})} \\ &= 1 - \frac{\sum_{\mathbf{y} | S_{\mathbf{y}} \cap C \cap \bar{Q} \neq \emptyset} p(\mathbf{y})}{\sum_{\mathbf{y} | S_{\mathbf{y}} \cap C \neq \emptyset} p(\mathbf{y})} \\ \text{Pl}(Q | C) &= 1 - \text{Bel}(\bar{Q} | C) \\ &= \frac{\sum_{\mathbf{y} | S_{\mathbf{y}} \cap C \cap Q \neq \emptyset} p(\mathbf{y})}{\sum_{\mathbf{y} | S_{\mathbf{y}} \cap C \neq \emptyset} p(\mathbf{y})} \end{aligned} \quad (2)$$

2.2 Model definitions

I now define the full form of NBR by generalizing the previous section in a number of ways: R 's are replaced by fuzzy sets represented by neural networks; U becomes the latent space which is separated from observation space.

An NBR model has the following components and Figure 1 illustrates the architecture.

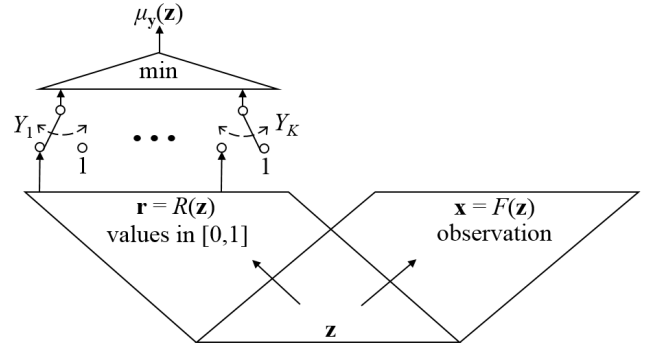


Figure 1: Architecture of NBR.

- Function $\mathbf{x} = F(\mathbf{z})$ where vector \mathbf{x} is the observation variables and vector \mathbf{z} is the latent variables.
- Function $\mathbf{r} = R(\mathbf{z})$ with output values in range $[0, 1]$.
- Bernoulli variables $\mathbf{Y} = (Y_1, Y_2, \dots, Y_K)$, where K is the dimension of \mathbf{r} .

The F and R functions can be implemented by neural networks. The parameters of an NBR model are the parameters of functions F and R , and $b_i = P_{Y_i}(1)$ for $i = 1, 2, \dots, K$.

Each $R_i(\mathbf{z})$ is interpreted as the membership function of a fuzzy set over \mathbf{z} space (Zadeh 1965). I consider the same 2^K possible worlds as in Section 2.1, but the intersection set $S_{\mathbf{y}}$ for each world now becomes the intersection of fuzzy sets and has the following membership function:

$$\mu_{\mathbf{y}}(\mathbf{z}) = \min_{i=1}^K (y_i \cdot R_i(\mathbf{z}) + 1 - y_i) \quad (3)$$

Consequently, the satisfiability of each world is no longer a binary property, but a degree in $[0, 1]$: $\max_{\mathbf{z}} \mu_{\mathbf{y}}(\mathbf{z})$. Therefore, the mass assigned to each world should be proportional to $p(\mathbf{y}) \cdot \max_{\mathbf{z}} \mu_{\mathbf{y}}(\mathbf{z})$. I still need to ensure that the total mass is one, and that leads to the following formula which replaces (1) as the new basic probability assignment.

$$m(S_{\mathbf{y}}) \triangleq \frac{p(\mathbf{y}) \cdot \max_{\mathbf{z}} \mu_{\mathbf{y}}(\mathbf{z})}{\sum_{\mathbf{y}'} (p(\mathbf{y}') \cdot \max_{\mathbf{z}} \mu_{\mathbf{y}'}(\mathbf{z}))} \quad (4)$$

Considering that $p(\cdot)$ is exactly the probability function of the Bernoulli vector \mathbf{Y} , the above has a more concise form:

$$m(S_{\mathbf{y}}) \triangleq \frac{p(\mathbf{y}) \cdot \max_{\mathbf{z}} \mu_{\mathbf{y}}(\mathbf{z})}{\mathbb{E}[\max_{\mathbf{z}} \mu_{\mathbf{Y}}(\mathbf{z})]} \quad (5)$$

With this new $m(\cdot)$ function, a belief function is specified over the \mathbf{z} space. The mapping from $m(\cdot)$ to $\text{Bel}(\cdot)$ is also generalized to handle fuzzy sets and is in Appendix A.2. Since \mathbf{x} is a deterministic function of \mathbf{z} , a belief function over the \mathbf{x} space is also implicitly specified.

2.3 Query answering

The most general form of a query is a conditional belief function given a condition function $C(\mathbf{z})$ which outputs a scalar in range $[0, 1]$. In an application, the condition likely comes as a function of \mathbf{x} , and since \mathbf{x} is a deterministic function of \mathbf{z} , $C(\mathbf{z})$ is the general form. The condition is classical

¹Proof is in Appendix A.1.

if $C(\mathbf{z})$ is Boolean, otherwise it is fuzzy and $C(\mathbf{z})$ is essentially the membership function of a fuzzy set over \mathbf{z} space.

To answer a general query, I simply add $C(\mathbf{z})$ as an extra entry to \mathbf{r} , and add a constant 1 as an extra entry to vector \mathbf{Y} . Intuitively, the NBR now has an additional rule that always exist. After such additions, the same formula (5) specifies a conditional belief function.

Let us now consider a special type of queries that are perhaps the most common in practice: given a Boolean function $C(\mathbf{z})$ as condition, compute the conditional belief and plausibility of a classical proposition, i.e., another Boolean function $Q(\mathbf{z})$. In other words, I will derive the replacement of (2) in a general NBR. Because S_Y is a fuzzy set specified by (3) while $C(\mathbf{z})$ is a classical set, the constraint of $S_Y \cap C \neq \emptyset$ is no longer binary but a degree in $[0, 1]$ and can be written as $\max_{\mathbf{z}|C(\mathbf{z})=1} \mu_Y(\mathbf{z})$. Therefore, the denominator in both formulas in (2) becomes $\sum_Y (p(\mathbf{y}) \cdot \max_{\mathbf{z}|C(\mathbf{z})=1} \mu_Y(\mathbf{z}))$. Applying the same to other terms in (2), and again utilizing the fact that $p(\cdot)$ is the probability function of \mathbf{Y} , I have the following formulas for conditional belief and plausibility for classical condition and proposition in a general NBR:

$$\text{Bel}(Q(\cdot) | C(\cdot)) = 1 - \frac{\text{E} \left[\max_{\mathbf{z}|C(\mathbf{z})=1, Q(\mathbf{z})=0} \mu_Y(\mathbf{z}) \right]}{\text{E} \left[\max_{\mathbf{z}|C(\mathbf{z})=1} \mu_Y(\mathbf{z}) \right]} \quad (6)$$

$$\text{Pl}(Q(\cdot) | C(\cdot)) = \frac{\text{E} \left[\max_{\mathbf{z}|C(\mathbf{z})=1, Q(\mathbf{z})=1} \mu_Y(\mathbf{z}) \right]}{\text{E} \left[\max_{\mathbf{z}|C(\mathbf{z})=1} \mu_Y(\mathbf{z}) \right]} \quad (7)$$

2.4 Sample generation

A belief function allows sample generation only if it is also a probability function, – recall that probability functions are a special case of belief functions (Shafer 1976). When combining two belief functions where one of the two is a probability function, by Dempster’s rule of combination (Shafer 1976), the resulting belief function is always a probability function. Therefore, to generate observation samples like traditional generative models, I combine the belief function of an NBR with a probability function over the \mathbf{x} space. This probability function is referred to as the *prior-knowledge distribution*. Intuitively, the prior-knowledge distribution represents assumptions or knowledge that are not included in this NBR. For example, if one only knows the range of \mathbf{x} , a uniform prior-knowledge distribution could be used; if one knows the mean and variance of \mathbf{x} , a Gaussian distribution could be used. As will become evident later, I only require the ability to draw samples from it. The flexibility to combine an NBR with various prior-knowledge distributions is analogous to applying the same knowledge in multiple environments. Section 2.5 will discuss more on the role of prior-knowledge distributions.

For clarity of presentation, let us focus on the scenario where the \mathbf{x} space is discrete. For a sample value $\tilde{\mathbf{x}}$, let $P_0(\tilde{\mathbf{x}})$ denote its probability in the prior-knowledge distri-

butions. Its probability after combining with an NBR is²

$$P(\mathbf{x} = \tilde{\mathbf{x}}) = \frac{P_0(\tilde{\mathbf{x}}) \cdot \text{Pl}(\mathbf{x} = \tilde{\mathbf{x}})}{\sum_{\mathbf{x}'} (P_0(\mathbf{x}') \cdot \text{Pl}(\mathbf{x} = \mathbf{x}'))} \quad (8)$$

where the plausibilities are given by (7) with C being always true. To generate samples according to (8), I simply draw samples from the prior-knowledge distribution and randomly keep or discard a sample, such that the probability to keep sample $\tilde{\mathbf{x}}$ is proportional to $\text{Pl}(\mathbf{x} = \tilde{\mathbf{x}})$. Note that the denominator in (7) does not change with Q and hence is the same for all $\tilde{\mathbf{x}}$ values; therefore I can simply use the numerator. In summary, the probability to keep a sample $\tilde{\mathbf{x}}$ drawn from the prior-knowledge distribution is:

$$P_{\text{keep}}(\tilde{\mathbf{x}}) = \text{E} \left[\max_{\mathbf{z}|F(\mathbf{z})=\tilde{\mathbf{x}}} \mu_Y(\mathbf{z}) \right]. \quad (9)$$

When the \mathbf{x} space is continuous, the generation procedure is the same: draw samples from a continuous prior-knowledge distribution and randomly keep or discard a sample according to the keep probability of (9).

2.5 Training

For unsupervised learning, an NBR is trained by maximizing the likelihood of observations in the sample generation process of the previous section. Therefore I need to choose a prior-knowledge distribution for training. This choice defines what should be learned by the NBR: information that is present in the observations yet that is beyond what is already encoded in the prior-knowledge distribution. For example, samples generated by an existing NBR can be used as the prior-knowledge distribution, and then the new NBR would be trained to learn and only learn knowledge that is beyond that existing NBR. Note that, after an NBR is trained, the query-answering process of Section 2.3 is independent of the prior-knowledge distribution used in training. In other words, an NBR’s answers are based on only the knowledge contained in itself, and this allows knowledge learned in one environment to be used in a different environment.

Given observations $\mathbf{x}_1, \dots, \mathbf{x}_n$, the likelihood loss is

$$\begin{aligned} \mathcal{L} &= -\frac{1}{n} \sum_{i=1}^n \log P(\mathbf{x} = \mathbf{x}_i) \\ &= -\frac{1}{n} \sum_{i=1}^n \log \frac{P_0(\mathbf{x}_i) \cdot P_{\text{keep}}(\mathbf{x}_i)}{\sum_{\mathbf{x}'} (P_0(\mathbf{x}') \cdot P_{\text{keep}}(\mathbf{x}'))} \\ &= -\frac{1}{n} \sum_{i=1}^n \log P_0(\mathbf{x}_i) - \frac{1}{n} \sum_{i=1}^n \log P_{\text{keep}}(\mathbf{x}_i) \\ &\quad + \log \sum_{\mathbf{x}'} (P_0(\mathbf{x}') \cdot P_{\text{keep}}(\mathbf{x}')) \end{aligned} \quad (10)$$

The first term is a constant and can be removed; the last term can be shortened by letting \mathbf{X} denote a vector of random variables that has the prior-knowledge distribution. The loss function becomes:

$$\mathcal{L} = -\frac{1}{n} \sum_{i=1}^n \log P_{\text{keep}}(\mathbf{x}_i) + \log \text{E}[P_{\text{keep}}(\mathbf{X})] \quad (11)$$

²Proof is in Appendix A.3.

Each training iteration uses a batch of observations to approximate the first term and a batch of samples from the prior-knowledge distribution to approximate the second term. There is an implementation issue with the second term: the expectation is before log, and with small batch size there is bias in gradient estimation. In practice, I use the following loss instead:

$$\mathcal{L} = -\frac{1}{n} \sum_{i=1}^n \log P_{\text{keep}}(\mathbf{x}_i) + \text{E}[P_{\text{keep}}(\mathbf{X})] / \alpha \quad (12)$$

where α is a constant that gets updated once every certain number of batches, and its value is an estimate of $\text{E}[P_{\text{keep}}(\mathbf{X})]$ on a large number of samples. It is straightforward to verify that, with a large batch size, (11) and (12) result in asymptotically the same gradients with respect to model parameters. The benefit of (12) is that the expectation in the second term is exposed and now small batch size can be used without causing bias in gradient estimation.

3 Unsupervised Learning: a Synthetic Task

This section gives a first demonstration of NBR on an unsupervised-learning task. Source code for training and inference is available at

<http://researcher.watson.ibm.com/group/10228>

Consider a world with 11 bits. Partial observations are available that observe either the first 10 bits or the last 10 bits. In observations of the first 10 bits, the first bit is the majority function of the middle 9 bits for 90% of the cases, and the inverse for 10% of the cases. In observations of the last 10 bits, the last bit is the majority function of the middle 9 bits for 20% of the cases, and the inverse for 80%.

An NBR is trained on these observations: K is 2; $F(\cdot)$ is identity function; $R(\cdot)$ is two three-layer ReLU networks, where each network is followed by a sigmoid unit, and where one network takes the first 10 bits as input and the other takes the last 10 bits. The loss function (12) is used, and the prior-knowledge distribution is uniform distribution over the 2^{11} possibilities. For a partial observation \mathbf{x}_i , let $\mathbf{x}_{i,0}$ and $\mathbf{x}_{i,1}$ be the two possible full observations. Substituting $P(\mathbf{x} = \mathbf{x}_i) = P(\mathbf{x} = \mathbf{x}_{i,0}) + P(\mathbf{x} = \mathbf{x}_{i,1})$ into (10) and following the same derivation to (12), it is straightforward to see that I simply need to compute $P_{\text{keep}}(\mathbf{x}_i)$ in (12) as $P_{\text{keep}}(\mathbf{x}_{i,0}) + P_{\text{keep}}(\mathbf{x}_{i,1})$.

Table 1 lists NBR’s answers to five sample queries. The belief values are computed by (6) and the plausibility values are by (7). In the first query, the condition is the first bit being 1 and the query is on the last bit. NBR answers with belief zero and plausibility 0.33, which means that it has some evidence to support x_{10} being 0 but no evidence to support x_{10} being 1. This answer is intuitive: with $x_0 = 1$, it is likely that the majority of the middle 9 bits is 1, and consequently it is likely that x_{10} is 0. Recall that during training the NBR has never seen an observation that simultaneously shows x_0 and x_{10} , and it answers the query by performing multi-hop reasoning with uncertainty. The second query is the opposite: with $x_0 = 0$, NBR has some evidence to support x_{10} being 1 but no evidence to support x_{10} being 0. There is an interesting comparison between the third and fourth queries: NBR’s

Table 1: Answers to example queries by NBR.

C	Q	belief	plausibility
$x_0 = 1$	x_{10}	0	0.33
$x_0 = 0$	x_{10}	0.67	1
$x_0 = 1, x_{1-4} = 0$	x_5	0.89	1
$x_0 = 1, x_{1-4} = 0, x_{10} = 1$	x_5	0.67	1
$x_0 = 1, x_{1-4} = 0, x_{6-10} = 1$	x_5	0.67	0.75

belief decreases when $x_{10} = 1$ is added to the condition. The reason is that $x_0 = 1$ and $x_{10} = 1$ are two conflicting pieces of information, and as a result the denominator in (6) is reduced to less than 1 for the fourth query, which in turn causes the belief value to decrease. This is consistent with human intuition when facing conflicting information. The fifth query is a similar case of conflicting information where all bits but x_5 are fixed. NBR’s answer means that it has evidence to support both possibilities for x_5 and that the evidence for x_5 being 1 is stronger than the evidence for 0. This is again consistent with human intuition based on observations of this world. It’s worth noting that the gap between belief and plausibility narrows for the fifth query, which reflects more information about the world from the condition, however the gap still exists, which reflects epistemic uncertainty, – the fact that NBR does not have complete knowledge about the world. The gap only closes when an NBR has complete knowledge regarding a query, in which case the answer would become a probability function.

To demonstrate the separation between latent space and observation space, a second NBR model is trained with non-trivial $F(\cdot)$. First an autoencoder is trained with a latent space of dimension 8. I then use the decoder part as $F(\cdot)$ and fix it as non-trainable during NBR training. When I need to evaluate the max operation in (9), I feed $\tilde{\mathbf{x}}$ into the encoder part to compute \mathbf{z} as a cheap surrogate operation. The resulting NBR gives the same answers as in Table 1.

4 Supervised Learning: a Robust MNIST Classifier

This section demonstrates NBR for supervised learning, and specifically discusses a robust MNIST classifier.

4.1 Using NBR for classification

It is possible to convert a classification task to unsupervised learning by treating training labels as part of the observation. However that is not the most efficient way to use NBR for classification, and this section presents a better approach. The discussion is on MNIST but most techniques are applicable to classification in general.

Given an MNIST image, let’s consider a world with 10 possibilities, – one of the ten labels is true. Recall from Section 2.2 that, in an NBR, the role of each entry in \mathbf{r} is to specify a fuzzy set. In a world with 10 possibilities, a fuzzy set is defined by 10 grades of membership, i.e., simply 10 numbers between 0 and 1. Therefore, each entry in \mathbf{r} can be implemented by an arbitrary MNIST classifier, and I simply add 10 sigmoid units at the end to convert logits to output

values in $[0, 1]$. Function $F(\cdot)$ is identity function and in fact will not be used. In summary, an NBR classifier is composed of \mathbf{r} , which is K classifiers with sigmoids added, and Bernoulli variables \mathbf{Y} .

Now let's define its outputs. With (6)(7), the belief and plausibility of each label can be computed; let them be Bel_j , Pl_j , $j \in \{0, \dots, 9\}$. I use this output vector:

$$\mathbf{o} = (\log \text{Pl}_0, \dots, \log \text{Pl}_9) \quad (13)$$

and its argmax is NBR's output label. The values in (13) are the negative of weights of evidence against each label (Shafer 1976). There are other choices: I could use $-\log(1 - \text{Bel}_j)$ which is the weight of evidence for label j (Shafer 1976), or use $\log \text{Pl}_j - \log(1 - \text{Bel}_j)$ which combines weights of evidence for and against label j . I choose (13) for computational efficiency.

Given an MNIST image, consider the fuzzy set specified by one entry in \mathbf{r} . It is possible, in fact often, that all grades of membership are below 1. In such a scenario, intuitively there is conflicting information within this rule itself: none of the possibilities is a full member of this fuzzy set. Although the NBR formulas can handle such rules as they are, it's beneficial to resolve such scenarios before computing (13) via (7). For a given image, let $\max(\mathbf{r}_i)$ denote the largest grade of membership from the i^{th} rule; I simply divide all grades of membership from the i^{th} rule by $\max(\mathbf{r}_i)$ and multiply b_i with $\max(\mathbf{r}_i)$. Intuitively, if a rule is conflicted on an image, the belief in it is reduced accordingly. Note that this scaling is different per image, and hence the now scaled b_i values vary by image. This operation is in a similar vein to the scaling step in Dempster's rule of combination, and I refer to it as *Dempster-style scaling*. Section 4.4 discusses its role in robustness.

4.2 Frames of discernment

Dempster's rule of combination assumes that sources represent entirely distinct bodies of evidence (Shafer 1976). Hence the K classifiers that constitute \mathbf{r} ought to learn different knowledge than each other. I achieve this by using different frames of discernment on them, and training those that share the same frame of discernment on different data.

Our implementation uses $K = 46$ rules, and Table 2 lists the 46 frames of discernment. To explain by example, let us consider the rule that has this frame of discernment: $\{0\} \{5,6\} \{7\}$. It is built as a classifier with 3 classes; for an image, let its three outputs after sigmoid be v_1 , v_2 and v_3 , and let $\hat{v} = \max(v_1, v_2, v_3)$. Then it specifies a fuzzy set with the following grades of membership for the 10 labels:

$$\frac{v_1}{\hat{v}}, 1, 1, 1, 1, \frac{v_2}{\hat{v}}, \frac{v_2}{\hat{v}}, \frac{v_3}{\hat{v}}, 1, 1$$

Note that the grades of membership for labels outside its frame of discernment, $\{1,2,3,4,8,9\}$, are always 1; intuitively this rule makes no judgment about them and considers those labels perfectly plausible. Also note that the grades of membership for 5 and 6 are always the same; intuitively this rule does not distinguish between them. In the above, I have applied Dempster-style scaling, and the b_i value for this rule for this image is multiplied with \hat{v} .

Table 2: Frames of discernment in NBR MNIST classifier.

{4} {9}	{5} {8}	{2} {8}	{2} {6}	{3,5} {4}
{4} {9}	{5} {8}	{8} {9}	{5} {6}	{0,2,6} {9}
{4} {9}	{3} {5}	{8} {9}	{4} {6}	{0,6} {1} {3}
{7} {9}	{3} {5}	{0} {2}	{2} {4}	{0} {5,6} {7}
{7} {9}	{3} {5}	{0} {2}	{3} {9}	{0} {1} {4}
{7} {9}	{3} {8}	{0} {6}	{1} {7}	{1} {5} {9}
{4} {7}	{3} {8}	{0} {6}	{2} {7}	{0,6} {8}
{4} {7}	{3} {8}	{1} {6}	{3} {7}	{1,4,7} {8}
{4} {7}	{2} {3}	{1} {6}		
{5} {8}	{2} {5}	{1} {2}		

Frames of discernment specify what knowledge each entry in \mathbf{r} learns from the training data. An obvious way to choose them is letting them be all pairs of labels, and the reason for those in the last column of Table 2 is to reduce K and reduce computational cost.

The reason for duplicates in Table2 is that those frames of discernment are difficult to learn robustly and hence multiple rules are needed to do the job. For example, 4 and 9 are perhaps the most difficult pair to distinguish and three rules are used on this pair. For rules that share the same frame, training data are split among them so that they learn different knowledge, and this will be discussed in the next section.

4.3 Loss functions for robustness

Each of the 46 classifiers that constitute \mathbf{r} is implemented as sigmoid ($s_i \cdot G_i(\text{image})$), where s_i is a scalar trainable parameter and $G_i(\cdot)$ is an L_2 -nonexpansive neural network (L2NNN) (Qian and Wegman 2019). Hence the overall trainable parameters are the parameters of $G_i(\cdot)$, s_i and b_i , for $i = 1, \dots, 46$. The training process has two steps. First, all $G_i(\cdot)$'s are trained: ones that share the same frame of discernment are trained jointly, while others are trained individually. Second, the NBR is trained as a whole but with only s_i 's and b_i 's being trainable; the reason for freezing $G_i(\cdot)$'s is to maintain them as distinct bodies of evidence. I now present loss functions used in the two steps.

For the first step, when multiple $G_i(\cdot)$'s are trained jointly, they only influence each other through training data splitting which gets updated once every certain number of batches, and the loss function is independent for each individual $G_i(\cdot)$. Let the i^{th} frame of discernment be $\Lambda_{i,1}, \dots, \Lambda_{i,J_i}$ where each $\Lambda_{i,j}$ is a set of labels. Let $T_{i,j}$ denote the set of training data with labels in $\Lambda_{i,j}$ and that are assigned to $G_i(\cdot)$; note that $T_{i_1,j} \cap T_{i_2,j} = \emptyset$ if the i_1^{th} and i_2^{th} frames of discernment are identical. Let $\bar{T}_{i,j}$ denote all training data with labels in $\bigcup_{1 \leq j' \leq J_i | j' \neq j} \Lambda_{i,j'}$. The loss function for training $G_i(\cdot)$ is:

$$\begin{aligned} \mathcal{L}_i = & \sum_{j=1}^{J_i} \text{avg}_{\mathbf{t} \in T_{i,j}} l \left(\text{ReLU} \left(\beta - G_i(\mathbf{t}) \right) \right) \\ & + \gamma \cdot \sum_{j=1}^{J_i} \text{avg}_{\mathbf{t} \in \bar{T}_{i,j}} l \left(\text{ReLU} \left(\beta + G_i(\mathbf{t}) \right) \right) \end{aligned} \quad (14)$$

where $l(\cdot)$ is a scalar penalty function; $\beta > 0$ and $\gamma \geq 1$ are hyperparameters. Intuitively, $G_i(\cdot)$ is penalized if its logit

for the correct $\Lambda_{i,j}$ is less than β or if the logits for the incorrect $\Lambda_{i,j}$'s are greater than $-\beta$. β controls the robustness-accuracy trade-off. γ controls the balance between the two types of penalties. Our implementation uses

$$l(a) = \min\left(\frac{a^2}{2 \cdot \eta}, \frac{\eta}{2}\right) + \text{ReLU}(a - \eta) + \omega \cdot \text{ReLU}(a - \xi) \quad (15)$$

where η, ω and ξ are hyperparameters. (15) is a heuristic and can be replaced by any increasing and convex function.

Once every certain number of batches, $T_{i,j}$'s are updated: among $G_i(\cdot)$'s that share the same frame of discernment, training images are re-assigned such that they incur less penalty in (14), subject to size lower bound for $T_{i,j}$'s which is imposed for training stability. Intuitively, a training image \mathbf{t} tends to be assigned to a $G_i(\cdot)$ that classifies \mathbf{t} the most robustly. Note that $\bar{T}_{i,j}$'s are constant and never updated.

In the second step, I train s_i 's and b_i 's through a technique called *poor man's adversarial training*. It is a cheap operation of decreasing the logit of each $G_i(\cdot)$ for the correct $\Lambda_{i,j}$ by τ while increasing the logits for the incorrect $\Lambda_{i,j}$'s by τ , where τ is a hyperparameter. Intuitively, because $G_i(\cdot)$'s are L2NNs, this operation is assuming the worst case scenario of an adversarial attack of L_2 distortion of τ . Let \mathbf{o}_{adv} denote the NBR output vector (13) under this assumption. For a training image \mathbf{t} , let $g_{\text{adv}}(\mathbf{t})$ denote the difference between the entry in \mathbf{o}_{adv} that corresponds to the correct label and its greatest entry for an incorrect label, and let $g_{\text{ori}}(\mathbf{t})$ denote the same for the original (13); classification is correct when g is positive. The loss function for the second step is:

$$\mathcal{L} = \text{avg}_{\mathbf{t}} (\text{sigmoid}(-g_{\text{adv}}(\mathbf{t}) \cdot \chi)) + \nu \cdot \text{avg}_{\mathbf{t}} (\text{sigmoid}(-g_{\text{ori}}(\mathbf{t}) \cdot \chi)) \quad (16)$$

where χ, ν are hyperparameters. (16) is a heuristic and one can derive other loss functions based on \mathbf{o}_{adv} and (13).

4.4 Proof of asymptotic robustness

For a training image \mathbf{t} , let $d(\mathbf{t})$ denote the distance from \mathbf{t} to the nearest training image with a different label. There exists a classifier that has 100% accuracy on the training set, and, for each \mathbf{t} , outputs the same label within a ball of radius $d(\mathbf{t})/2$ around \mathbf{t} . I refer to this as the *oracle robustness* as it is the best achievable on a given training set. For the MNIST training set and for L_2 distance, the oracle robustness radius is above 3 for 51% of images, above 2.5 for 79% of images, and above 2 for 96% of images. Consequently, it is arguable that $\varepsilon = 2$ is the meaningful L_2 threshold when quantifying robustness of MNIST classifiers, because measuring with a higher ε could introduce the possibility of a biased classifier that favors a subset of images.

This section uses the L_2 metric. Although the same argument applies to other metrics, there is only practical significance in L_2 because there are not yet known efficient ways to build nonexpansive neural networks for other metrics.

Theorem 1. *For any constant $\delta > 0$, there exists an NBR classifier that classifies each training datum \mathbf{t} correctly within a ball of L_2 radius $d(\mathbf{t})/2 - \delta$.*

Proof. Without loss of generality, let us consider a task with two classes, A and B. For all $G_i(\cdot)$'s, the frame of discernment is the same: $\{A\} \cup \{B\}$. Consider the extreme case that each $T_{i,j}$ contains exactly one training datum. Then $G_i(\cdot)$ has a trivial implementation: the first logit is $G_i(\mathbf{t})_1 = d(\hat{\mathbf{t}}_i)/2 - \|\mathbf{t} - \hat{\mathbf{t}}_i\|_2$ where $\hat{\mathbf{t}}_i$ is the only member of $T_{i,1}$, and the second logit is similar.

Consider a training datum \mathbf{t} with label A, and let $T_{i_t,1}$ be the subset that contains it. I have $G_{i_t}(\mathbf{t})_1 = d(\mathbf{t})/2$ and $G_i(\mathbf{t})_2 \leq -d(\mathbf{t})/2, \forall i$, proof in Appendix A.4.

Hence for any \mathbf{t}' such that $\|\mathbf{t}' - \mathbf{t}\|_2 \leq d(\mathbf{t})/2 - \delta$, it must be true that $G_{i_t}(\mathbf{t}')_1 \geq \delta$ and $G_i(\mathbf{t}')_2 \leq -\delta, \forall i$. Obviously $G_{i_t}(\cdot)$ classifies correctly. Some others could misclassify: in such a rule, it must be true that $G_i(\mathbf{t}')_1 < G_i(\mathbf{t}')_2 \leq -\delta$. Therefore the grades of membership before Dempster-style scaling are $\text{sigmoid}(s_i \cdot G_i(\mathbf{t}')_1) < \text{sigmoid}(s_i \cdot G_i(\mathbf{t}')_2) \leq \text{sigmoid}(-s_i \cdot \delta)$. Therefore Dempster-style scaling multiplies b_i with the grade of membership for B, which is no greater than $\text{sigmoid}(-s_i \cdot \delta)$. s_i can be arbitrarily large in this NBR, and hence the scaled b_i can be arbitrarily small for \mathbf{t}' and this rule has little effect in (7). This argument applies to any $G_i(\mathbf{t}')$ that misclassifies. Therefore, with sufficiently large s_i 's, this NBR always classifies \mathbf{t}' as label A. \square

The NBR in the proof is neither practical, due to an extremely large K , nor desirable because it memorizes training data. However, there is a continuous spectrum of NBRs as K varies, and the sweet spot is likely in the middle: when the $T_{i,j}$'s are meaningful subsets of data, an NBR might reach the best combination of robustness and generalization.

4.5 Results

The NBR MNIST classifier is available at <http://researcher.watson.ibm.com/group/10228>

Table 3 compares the NBR MNIST classifier against those in (Madry et al. 2018; Wong and Kolter 2018; Qian and Wegman 2019), all of which are publicly available. Among them, the L2NN classifier from (Qian and Wegman 2019) is the state of the art in robustness as measured by L_2 metric.

The robust accuracies are measured on the first 1000 images in the MNIST test set by running four attacks: projected gradient descent (PGD) (Madry et al. 2018), boundary attack (Brendel, Rauber, and Bethge 2018), Carlini & Wagner (CW) attack (Carlini and Wagner 2017b) and seeded CW. Foolbox (Rauber, Brendel, and Bethge 2017) is used for PGD and boundary attacks; CW is original code from (Carlini and Wagner 2017b); seeded CW is a CW search with a starting point that is provided by a transfer attack, and is a straightforward variation of the CW code. Iteration limit is 100 for PGD, 50K for boundary attack, and 10K for CW and seeded CW. More details are in Appendix B. As discussed in Section 4.4, $\varepsilon = 2$ is a meaningful L_2 threshold for MNIST. A classifier is considered robust on an image if it remains correct under all four attacks.

Table 3 shows that the NBR classifier has the best robustness, and at the same time the best natural accuracy among all but the non-robust vanilla model. I do not have access to the model in (Schott et al. 2019) and can only compare with

Table 3: Accuracies on natural images and on adversarial images where the L_2 -norm limit of distortion is 2.

	natural	robust
Vanilla	99.1%	0%
Madry et al.	98.5%	3.3%
Wong&Kolter	98.8%	8.9%
L2NNN	98.2%	61.2%
NBR	99.0%	61.6%

Table 4: Accuracies on out-of-distribution images.

	thin	framed
Vanilla	88.5%	85.3%
Madry et al.	97.3%	82.7%
Wong&Kolter	97.1%	91.6%
L2NNN	95.7%	98.3%
NBR	97.6%	98.8%

reported numbers: their natural accuracy is 99% and robust accuracy is 80% for L_2 threshold of 1.5. For 1.5, the NBR classifier has a robust accuracy of 83.5%. It’s worth noting that the NBR model is end-to-end differentiable while the model of (Schott et al. 2019) is not, and hence our 83.5% is likely after more scrutiny from attacks than their 80%.

Ablation studies are in Appendix C and include classifiers in which belief-function arithmetic is replaced by Markov random field and Gaussian naive Bayes.

Another hypothesis is that a model with reasoning ought to generalize better on out-of-distribution data points. I derived two data sets from the MNIST test set: thin-MNIST, in which many pixels are set to zero based on each pixel’s neighborhood information, and framed-MNIST, in which the boundary pixels are set to one. Generation scripts are available at the link at the beginning of this section. Sample images are shown in Figure 2. Table 4 compares various models on these out-of-distribution images, and NBR outperforms the rest.

5 Related Work

As a formalism for reasoning with uncertainty, belief functions (Shafer 1976) have two distinct advantages: explicit modeling of the lack of knowledge and an elegant mechanism of combining multiple sources of information. Consequently reasoning frameworks based on belief functions have been proposed (Gordon and Shortliffe 1985; Baldwin 1986; Lowrance, Garvey, and Strat 1986; Laskey and Lehner 1988; D’Ambrosio 1988; Wan and Kifer 2009), and they have varying degrees of similarity to the restricted framework of Section 2.1. These early works share some common weaknesses in practice: where do rules come from, and where do uncertainty quantifications on the rules come from. Relying on manual inputs is clearly not scalable.³ To be

³Another reason for limited adoption of belief function is criticism in literature, e.g., (Pearl 1990). I disagree with much of

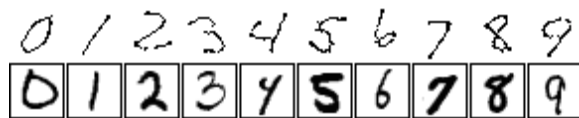


Figure 2: Sample thin-MNIST and framed-MNIST images. Color is inverted to make frames visible.

fair, mainstream methods based on Bayesian network (Pearl 1988) or Markov random field (Kindermann and Snell 1980) often have the same weaknesses. Some have addressed the second weakness: for example, Markov logic networks (Richardson and Domingos 2006) learn the weights on clauses. Attempts to address the first weakness, e.g., by inductive logic programming (Muggleton and De Raedt 1994; De Raedt and Kersting 2008), are often limited.

Progresses in addressing the first weakness via automatic discovery of rules have emerged from the machine learning field. In (Hinton 2002; Salakhutdinov and Hinton 2009), Markov-random-field models, which can be viewed as compositions of non-symbolic rules, are learned from data. In (França, Zaverucha, and Garcez 2014; Evans and Grefenstette 2018), symbolic logic programs are learned from examples by neural networks. Another example is (Serafini and Garcez 2016) which defines a formalism of real-valued logic and thereby enables learning non-symbolic rules.

Adversarial robustness is a well-known difficult problem (Szegedy et al. 2014; Goodfellow, Shlens, and Szegedy 2015; Carlini and Wagner 2017b), and many remedies have been tried and failed (Carlini and Wagner 2017a; Athalye, Carlini, and Wagner 2018). For MNIST, if distortion is measured by the L_∞ distance, there are a number of approaches (Wong and Kolter 2018; Raghunathan, Steinhardt, and Liang 2018; Schott et al. 2019) and in particular (Madry et al. 2018) achieves good L_∞ robustness by adversarial training. For L_2 robustness which is less understood and perhaps more difficult, before this work the state of the art is an L2NNN from (Qian and Wegman 2019) with adversarial training. It’s worth noting that adversarial training alone does not work well for L_2 robustness (Schott et al. 2019; Qian and Wegman 2019; Tsipras et al. 2019). One hypothesis in this paper is that reasoning is a missing piece in previous works on robustness.

6 Conclusions and Future Work

This paper presents neural belief reasoner, which is a new generative model and a new approach to combine learning and reasoning. Its properties are studied through two tasks: an unsupervised-learning task of reasoning with uncertainty, and a supervised-learning task of robust classification. In particular, the MNIST classifier sets a new state of the art in L_2 robustness while maintaining 99% nominal accuracy.

This paper only scratches the surface. As discussed in the text, both tasks use NBRs with certain restrictions, e.g., $F(\cdot)$

the criticism. A comparative study between belief function and Bayesian inference is beyond the scope of this paper; ablation studies in Appendix C do offer some empirical results.

being identity function. To unlock its full potential, innovations would be needed for efficient inference and training algorithms, including but not limited to Monte Carlo methods, as well as efficient constraint-programming solvers. There are also open questions from the application perspective, e.g., how to take advantage of NBR’s sample-generation capability and how to leverage NBR for interpretability.

References

- [Athalye, Carlini, and Wagner 2018] Athalye, A.; Carlini, N.; and Wagner, D. 2018. Obfuscated gradients give a false sense of security: Circumventing defenses to adversarial examples. In *International Conference on Machine Learning*.
- [Baldwin 1986] Baldwin, J. F. 1986. Support logic programming. In *Fuzzy sets theory and applications*. Springer. 133–170.
- [Brendel, Rauber, and Bethge 2018] Brendel, W.; Rauber, J.; and Bethge, M. 2018. Decision-based adversarial attacks: Reliable attacks against black-box machine learning models. In *International Conference on Learning Representations*.
- [Carlini and Wagner 2017a] Carlini, N., and Wagner, D. 2017a. Adversarial examples are not easily detected: Bypassing ten detection methods. In *Proceedings of the ACM Workshop on Artificial Intelligence and Security*, 3–14. ACM.
- [Carlini and Wagner 2017b] Carlini, N., and Wagner, D. 2017b. Towards evaluating the robustness of neural networks. In *Proceedings of the IEEE Symposium on Security and Privacy*, 39–57.
- [D’Ambrosio 1988] D’Ambrosio, B. 1988. A hybrid approach to reasoning under uncertainty. *International Journal of Approximate Reasoning* 2(1):29–45.
- [De Raedt and Kersting 2008] De Raedt, L., and Kersting, K. 2008. Probabilistic inductive logic programming. In *Probabilistic Inductive Logic Programming: Theory and Applications*. Springer. 1–27.
- [Evans and Grefenstette 2018] Evans, R., and Grefenstette, E. 2018. Learning explanatory rules from noisy data. *Journal of Artificial Intelligence Research* 61:1–64.
- [França, Zaverucha, and Garcez 2014] França, M. V.; Zaverucha, G.; and Garcez, A. d. 2014. Fast relational learning using bottom clause propositionalization with artificial neural networks. *Machine learning* 94(1):81–104.
- [Goodfellow, Shlens, and Szegedy 2015] Goodfellow, I. J.; Shlens, J.; and Szegedy, C. 2015. Explaining and harnessing adversarial examples. In *International Conference on Learning Representations*.
- [Gordon and Shortliffe 1985] Gordon, J., and Shortliffe, E. H. 1985. A method for managing evidential reasoning in a hierarchical hypothesis space. *Artificial intelligence* 26(3):323–357.
- [Hinton 2002] Hinton, G. E. 2002. Training products of experts by minimizing contrastive divergence. *Neural computation* 14(8):1771–1800.
- [Kindermann and Snell 1980] Kindermann, R., and Snell, J. L. 1980. *Markov Random Fields and Their Applications*. American Mathematical Society.
- [Laskey and Lehner 1988] Laskey, K. B., and Lehner, P. E. 1988. Belief maintenance: An integrated approach to uncertainty management. In *AAAI Conference on Artificial Intelligence*, 210–214.
- [Lowrance, Garvey, and Strat 1986] Lowrance, J. D.; Garvey, T. D.; and Strat, T. M. 1986. A framework for evidential-reasoning systems. In *AAAI Conference on Artificial Intelligence*, 896–901.
- [Madry et al. 2018] Madry, A.; Makelov, A.; Schmidt, L.; Tsipras, D.; and Vladu, A. 2018. Towards deep learning models resistant to adversarial attacks. In *International Conference on Learning Representations*.
- [Muggleton and De Raedt 1994] Muggleton, S., and De Raedt, L. 1994. Inductive logic programming: Theory and methods. *The Journal of Logic Programming* 19:629–679.
- [Pearl 1988] Pearl, J. 1988. *Probabilistic Reasoning in Intelligent Systems: Networks of Plausible Inference*. Morgan Kaufmann.
- [Pearl 1990] Pearl, J. 1990. Reasoning with belief functions: An analysis of compatibility. *International Journal of Approximate Reasoning* 4(5-6):363–389.
- [Qian and Wegman 2019] Qian, H., and Wegman, M. N. 2019. L2-nonexpansive neural networks. In *International Conference on Learning Representations*.
- [Raghunathan, Steinhardt, and Liang 2018] Raghunathan, A.; Steinhardt, J.; and Liang, P. 2018. Certified defenses against adversarial examples. In *International Conference on Learning Representations*.
- [Rauber, Brendel, and Bethge 2017] Rauber, J.; Brendel, W.; and Bethge, M. 2017. Foolbox: A python toolbox to benchmark the robustness of machine learning models. *arXiv preprint arXiv:1707.04131*.
- [Richardson and Domingos 2006] Richardson, M., and Domingos, P. 2006. Markov logic networks. *Machine learning* 62(1-2):107–136.
- [Salakhutdinov and Hinton 2009] Salakhutdinov, R., and Hinton, G. 2009. Deep Boltzmann machines. In *International Conference on Artificial Intelligence and Statistics*.
- [Schott et al. 2019] Schott, L.; Rauber, J.; Bethge, M.; and Brendel, W. 2019. Towards the first adversarially robust neural network model on MNIST. In *International Conference on Learning Representations*.
- [Serafini and Garcez 2016] Serafini, L., and Garcez, A. d. 2016. Logic tensor networks: Deep learning and logical reasoning from data and knowledge. *arXiv preprint arXiv:1606.04422*.
- [Shafer 1976] Shafer, G. 1976. *A Mathematical Theory of Evidence*. Princeton University Press.
- [Szegedy et al. 2014] Szegedy, C.; Zaremba, W.; Sutskever, I.; Bruna, J.; Erhan, D.; Goodfellow, I.; and Fergus, R. 2014. Intriguing properties of neural networks. In *International Conference on Learning Representations*.
- [Tsipras et al. 2019] Tsipras, D.; Santurkar, S.; Engstrom, L.; Turner, A.; and Madry, A. 2019. Robustness may be at odds with accuracy. In *International Conference on Learning Representations*.
- [Wan and Kifer 2009] Wan, H., and Kifer, M. 2009. Belief logic programming: uncertainty reasoning with correlation of evidence. In *Logic Programming and Nonmonotonic Reasoning, Lecture Notes in Computer Science*, 316–328.
- [Wong and Kolter 2018] Wong, E., and Kolter, Z. 2018. Provable defenses against adversarial examples via the convex outer adversarial polytope. In *International Conference on Machine Learning*.
- [Zadeh 1965] Zadeh, L. A. 1965. Fuzzy sets. *Information and Control* 8(3):338–353.

A Proofs

A.1 Proof of equation (2)

Proof. According to (Shafer 1976), conditional belief is

$$\begin{aligned} \text{Bel}(Q | C) &= \frac{\text{Bel}(Q \cup \bar{C}) - \text{Bel}(\bar{C})}{1 - \text{Bel}(\bar{C})} \\ &= 1 - \frac{1 - \text{Bel}(Q \cup \bar{C})}{1 - \text{Bel}(\bar{C})} \end{aligned} \quad (\text{A.1})$$

Substituting the mapping formula from $m(\cdot)$ to $\text{Bel}(\cdot)$, the formula becomes

$$\text{Bel}(Q | C) = 1 - \frac{1 - \sum_{B \subseteq Q \cup \bar{C}} m(B)}{1 - \sum_{B \subseteq \bar{C}} m(B)} \quad (\text{A.2})$$

Substituting (1) into the above, since the denominator in (1) is a constant, I can then multiply both the numerator and the denominator in (A.2) with it, and the formula becomes

$$\text{Bel}(Q | C) = 1 - \frac{1 - \sum_{\mathbf{y} | S_{\mathbf{y}} = \emptyset} p(\mathbf{y}) - \sum_{\mathbf{y} | S_{\mathbf{y}} \neq \emptyset, S_{\mathbf{y}} \subseteq Q \cup \bar{C}} p(\mathbf{y})}{1 - \sum_{\mathbf{y} | S_{\mathbf{y}} = \emptyset} p(\mathbf{y}) - \sum_{\mathbf{y} | S_{\mathbf{y}} \neq \emptyset, S_{\mathbf{y}} \subseteq \bar{C}} p(\mathbf{y})} \quad (\text{A.3})$$

It's straightforward to verify that $\sum_{\forall \mathbf{y}} p(\mathbf{y}) = 1$. Substituting the 1 in both the numerator and the denominator in (A.3) with this sum, the formula becomes

$$\begin{aligned} \text{Bel}(Q | C) &= 1 - \frac{\sum_{\mathbf{y} | S_{\mathbf{y}} \not\subseteq Q \cup \bar{C}} p(\mathbf{y})}{\sum_{\mathbf{y} | S_{\mathbf{y}} \not\subseteq \bar{C}} p(\mathbf{y})} \\ &= 1 - \frac{\sum_{\mathbf{y} | S_{\mathbf{y}} \cap C \cap \bar{Q} \neq \emptyset} p(\mathbf{y})}{\sum_{\mathbf{y} | S_{\mathbf{y}} \cap C \neq \emptyset} p(\mathbf{y})} \end{aligned} \quad (\text{A.4})$$

By now I have proved the first half of (2). The second half can be easily derived from the first half, by utilizing the relation between belief and plausibility (Shafer 1976):

$$\begin{aligned} \text{Pl}(Q | C) &= 1 - \text{Bel}(\bar{Q} | C) \\ &= 1 - \left(1 - \frac{\sum_{\mathbf{y} | S_{\mathbf{y}} \cap C \cap Q \neq \emptyset} p(\mathbf{y})}{\sum_{\mathbf{y} | S_{\mathbf{y}} \cap C \neq \emptyset} p(\mathbf{y})} \right) \\ &= \frac{\sum_{\mathbf{y} | S_{\mathbf{y}} \cap C \cap Q \neq \emptyset} p(\mathbf{y})}{\sum_{\mathbf{y} | S_{\mathbf{y}} \cap C \neq \emptyset} p(\mathbf{y})} \end{aligned} \quad (\text{A.5})$$

□

A.2 Mapping from $m(\cdot)$ to $\text{Bel}(\cdot)$ with fuzzy sets

For a classical set A , the formula for $\text{Bel}(A)$ is given by equation (6), with C being always true and Q being the Boolean membership function of A . Hence I only need to derive the equivalent of (6) for a fuzzy set A ; let $\mu_A(\mathbf{z})$ denote its membership function. With a fuzzy set, I can no longer take the max in the numerator of (6) under a hard condition of $\mu_A(\mathbf{z}) = 0$. That needs to be replaced by the max grade of membership in the intersection set between \bar{A} and each $S_{\mathbf{y}}$. Let $\mu_{S_{\mathbf{y}} \cap \bar{A}}(\mathbf{z}) = \min(\mu_{\mathbf{y}}(\mathbf{z}), 1 - \mu_A(\mathbf{z}))$

according to fuzzy set arithmetic (Zadeh 1965), and the belief on a fuzzy set is

$$\begin{aligned} \text{Bel}(A) &= 1 - \frac{\text{E} \left[\max_{\mathbf{z}} (\min(\mu_{\mathbf{y}}(\mathbf{z}), 1 - \mu_A(\mathbf{z}))) \right]}{\text{E} \left[\max_{\mathbf{z}} \mu_{\mathbf{y}}(\mathbf{z}) \right]} \\ &= 1 - \frac{\sum_{\mathbf{y}} p(\mathbf{y}) \cdot \max_{\mathbf{z}} \mu_{S_{\mathbf{y}} \cap \bar{A}}(\mathbf{z})}{\text{E} \left[\max_{\mathbf{z}} \mu_{\mathbf{y}}(\mathbf{z}) \right]} \end{aligned} \quad (\text{A.6})$$

Utilizing equation (5) and the fact that total mass assignment is 1, the above equation can be rewritten to the following.

$$\text{Bel}(A) = \sum_{\mathbf{y}} m(S_{\mathbf{y}}) \cdot \left(1 - \frac{\max_{\mathbf{z}} \mu_{S_{\mathbf{y}} \cap \bar{A}}(\mathbf{z})}{\max_{\mathbf{z}} \mu_{\mathbf{y}}(\mathbf{z})} \right) \quad (\text{A.7})$$

The above mapping from $m(\cdot)$ to $\text{Bel}(\cdot)$ is intuitive: the belief in a fuzzy set is a weighted sum of mass values assigned to each possible world, and each weight is a fraction value that depends on the satisfiability of $S_{\mathbf{y}} \cap \bar{A}$ as well as $S_{\mathbf{y}}$ itself. It's straightforward to verify that, if A and $S_{\mathbf{y}}$'s are all classical sets, equation (A.7) is identical to the classical mapping (Shafer 1976): $\text{Bel}(A) = \sum_{B \subseteq A} m(B)$.

A.3 Proof of equation (8)

Proof. For clarity of presentation, let us focus on the scenario where the \mathbf{x} space is discrete. Because Dempster's rule of combination is associative (Shafer 1976), combining an NBR and a prior-knowledge distribution is the same as combining $K + 1$ belief functions, where the first K are from the NBR while the last one is the prior-knowledge distribution. Let $m'(\cdot)$ denote the resulting basic probability assignment. By Dempster's rule of combination, $m'(\cdot)$ assigns mass to sets in the form of $S_{\mathbf{y}, \tilde{\mathbf{x}}} \triangleq S_{\mathbf{y}} \cap \{\mathbf{z} | F(\mathbf{z}) = \tilde{\mathbf{x}}\}$ where $\tilde{\mathbf{x}}$ is an element in the \mathbf{x} space. Let $\mu_{\mathbf{y}, \tilde{\mathbf{x}}}(\mathbf{z})$ denote the membership function of $S_{\mathbf{y}, \tilde{\mathbf{x}}}$. Obviously $\mu_{\mathbf{y}, \tilde{\mathbf{x}}}(\mathbf{z})$ is non-zero only where $F(\mathbf{z}) = \tilde{\mathbf{x}}$. Therefore, if I consider the implicitly specified belief function over the \mathbf{x} space, mass is only assigned to singletons, – sets with one and only one element; this is exactly the condition when a belief function becomes a probability function, and the probability of an outcome is the total mass assigned to the corresponding singleton. If $S_{\mathbf{y}}$'s are classical sets, the resulting probability from combining $K + 1$ sources is

$$\begin{aligned} P(\mathbf{x} = \tilde{\mathbf{x}}) &= \sum_{\mathbf{y}} m'(S_{\mathbf{y}, \tilde{\mathbf{x}}}) \\ &= \sum_{\mathbf{y}} \frac{P_0(\tilde{\mathbf{x}}) \cdot p(\mathbf{y}) \cdot \sigma_{S_{\mathbf{y}, \tilde{\mathbf{x}}}}}{\Xi} \end{aligned} \quad (\text{A.8})$$

where $P_0(\tilde{\mathbf{x}})$ is the probability of $\tilde{\mathbf{x}}$ in the prior-knowledge distributions, $\sigma_{S_{\mathbf{y}, \tilde{\mathbf{x}}}}$ is the Boolean satisfiability of $S_{\mathbf{y}, \tilde{\mathbf{x}}}$, and Ξ is a normalizing constant.

For fuzzy sets, I only need to replace $\sigma_{S_{\mathbf{y}, \tilde{\mathbf{x}}}}$ with a degree of satisfiability:

$$\max_{\mathbf{z}} \mu_{\mathbf{y}, \tilde{\mathbf{x}}}(\mathbf{z}) = \max_{\mathbf{z} | F(\mathbf{z}) = \tilde{\mathbf{x}}} \mu_{\mathbf{y}}(\mathbf{z}) \quad (\text{A.9})$$

Therefore the generalized form of (A.8) is

$$\begin{aligned}
P(\mathbf{x} = \tilde{\mathbf{x}}) &= \sum_{\mathbf{y}} \frac{P_0(\tilde{\mathbf{x}}) \cdot p(\mathbf{y}) \cdot \max_{\mathbf{z}|F(\mathbf{z})=\tilde{\mathbf{x}}} \mu_{\mathbf{Y}}(\mathbf{z})}{\Xi} \\
&= \frac{P_0(\tilde{\mathbf{x}}) \cdot \sum_{\mathbf{y}} \left(p(\mathbf{y}) \cdot \max_{\mathbf{z}|F(\mathbf{z})=\tilde{\mathbf{x}}} \mu_{\mathbf{Y}}(\mathbf{z}) \right)}{\Xi} \\
&= \frac{P_0(\tilde{\mathbf{x}}) \cdot \mathbb{E} \left[\max_{\mathbf{z}|F(\mathbf{z})=\tilde{\mathbf{x}}} \mu_{\mathbf{Y}}(\mathbf{z}) \right]}{\Xi}
\end{aligned} \tag{A.10}$$

Note that the expectation term matches the numerator in (7) with C being always true and Q being the Boolean proposition of $F(\mathbf{z}) = \tilde{\mathbf{x}}$. After substituting (7) and setting a proper Ξ , (A.10) can be converted to the form of (8). \square

A.4 Proof of logit bounds in Section 4.4

Proof. For the NBR used in the proof in Section 4.4, consider a training datum \mathbf{t} with label A. For any i , let $\tilde{\mathbf{t}}_i$ denote the only member of $T_{i,2}$, which has label B.

If $d(\tilde{\mathbf{t}}_i) \geq d(\mathbf{t})$, then it must be true that

$$\begin{aligned}
G_i(\mathbf{t})_2 &= d(\tilde{\mathbf{t}}_i) / 2 - \|\mathbf{t} - \tilde{\mathbf{t}}_i\|_2 \\
&\leq d(\tilde{\mathbf{t}}_i) / 2 - d(\tilde{\mathbf{t}}_i) \\
&= -d(\tilde{\mathbf{t}}_i) / 2 \\
&\leq -d(\mathbf{t}) / 2
\end{aligned} \tag{A.11}$$

If $d(\tilde{\mathbf{t}}_i) < d(\mathbf{t})$, then it must be true that

$$\begin{aligned}
G_i(\mathbf{t})_2 &= d(\tilde{\mathbf{t}}_i) / 2 - \|\mathbf{t} - \tilde{\mathbf{t}}_i\|_2 \\
&\leq d(\tilde{\mathbf{t}}_i) / 2 - d(\mathbf{t}) \\
&< d(\mathbf{t}) / 2 - d(\mathbf{t}) \\
&= -d(\mathbf{t}) / 2
\end{aligned} \tag{A.12}$$

\square

B Details of Robustness Evaluation

This section presents a detailed description of the robustness evaluation used for Table 3, as well as results from individual attacks in Table B.1.

Robust accuracies are measured on the first 1000 images in the MNIST test set due to limitation of computing resources.⁴ On each image and for each classifier, four attacks are performed:

- Projected gradient descent (PGD) (Madry et al. 2018): the implementation in Foolbox (Rauber, Brendel, and Bethge 2017) is used, with an iteration limit of 100. I observe empirically that, for L_2 attacks, PGD with 100 iterations outperforms PGD with 1000 iterations.
- Boundary attack (Brendel, Rauber, and Bethge 2018): the implementation in Foolbox (Rauber, Brendel, and Bethge 2017) is used, with an iteration limit of 50,000.

⁴Note that natural accuracies in Table 3 are measured on the whole test set, and so are all measurements in Table 4.

Table B.1: Accuracies on adversarial images where the L_2 -norm limit of distortion is 2. BA is boundary attack. SCW is seeded CW attack. Best is picking the best of four attacks for each image.

	PGD	BA	CW	SCW	best
Vanilla	45.7%	0%	0%	0%	0%
Madry et al.	96.6%	8.3%	56.2%	19.1%	3.3%
Wong&Kolter	95.8%	13.5%	66.6%	33.1%	8.9%
L2NNN	92.3%	79.5%	62.4%	61.3%	61.2%
NBR	89.4%	78.0%	72.8%	62.8%	61.6%

- Carlini & Wagner (CW) attack (Carlini and Wagner 2017b): the original code from (Carlini and Wagner 2017b) is used, with an iteration limit of 10,000.
- Seeded CW attack: a CW attack that starts each search from an image that is provided by a transfer attack. The implementation is a straightforward modification from the code of (Carlini and Wagner 2017b), and an iteration limit of 10,000 is used. The transfer attack is a CW attack on a modified NBR classifier in which all s_i values are reduced, and I simply save the adversarial images and load them during seeded CW attacks. Theoretically this transfer attack should produce starting points that are the most effective in attacking the NBR classifier. As shown in Table B.1, these starting points are also quite effective in attacking the classifiers from (Madry et al. 2018; Wong and Kolter 2018). I hypothesize that they are close to genuinely ambiguous images and hence are good starting points for CW attacks.

Per discussion in Section 4.4 on oracle robustness, $\varepsilon = 2$ is the meaningful L_2 threshold when quantifying robustness of MNIST classifiers. A classifier is considered robust on an image if it remains correct under all four attacks, i.e., if none of the four attacks is able to find an adversarial example within L_2 distance of 2.

One observation in Table B.1 is that the boundary attack is particularly powerful in attacking the classifiers from (Madry et al. 2018; Wong and Kolter 2018). Similar results on (Madry et al. 2018) have been reported in (Schott et al. 2019).

C Ablation Studies

The NBR MNIST classifier of Section 4 can be viewed as combining $K = 46$ sources of information, each of which is an L2NNN, and NBR is the method to combine them. From this perspective, an important question is: what other methods are there for performing the combination, and how do they compare with NBR? This section presents some empirical answers by building classifiers in which the 46 sources are kept the same while NBR’s combining operations are replaced by various approaches, including Markov random field (MRF) and Gaussian naive Bayes.

Table C.1 lists the natural accuracy and robust accuracy of the ablation-study models, which are measured in the same way as Table 3 and as described in the previous section. The first row is copied from Table 3 as a reference.

Table C.1: Accuracies of ablation-study models on natural images and on adversarial images where the L_2 -norm limit of distortion is 2.

	natural	robust
NBR	99.0%	61.6%
No Dempster-style scaling	97.6%	53.2%
Markov random field #1	98.6%	55.5%
Markov random field #1+	98.9%	57.2%
Markov random field #2	97.2%	54.1%
Gaussian naive Bayes #1	98.8%	54.1%
Gaussian naive Bayes #1+	98.0%	45.0%
Gaussian naive Bayes #2	97.6%	42.6%

- The second row is an NBR classifier without the step of Dempster-style scaling, which was discussed in Section 4.1; the s_i and b_i parameters are re-trained. Given the role that Dempster-style scaling plays in the robustness proof of Section 4.4, the drop in robustness is not surprising. The results suggest that Dempster-style scaling also contributes to the accuracy on natural images.
- The third, fourth and fifth rows are models that assume a Boltzmann distribution among the ten labels for a given image. I refer to them as MRF models because the formulas for MRF classifiers are used, in which each of the ten outputs is a weighted sum of energy functions, and also because the frames of discernment from Section 4.2 do form a graph structure for MRF. Trainable weight parameters w_1, \dots, w_{46} replace NBR’s b_1, \dots, b_{46} . For each of the three models, the s_i and w_i parameters are re-trained. There are two choices of energy functions: MRF #1 and MRF #1+ use $-\text{sigmoid}(s_i \cdot G_i(\text{image}))$, $i \in \{1, \dots, 46\}$, as energy functions, while MRF #2 uses $-\log(\text{sigmoid}(s_i \cdot G_i(\text{image})))$. The difference between MRF #1 and MRF #1+ is that a step is added in MRF #1+ that mimics Dempster-style scaling: the energy values from each energy function are scaled up as discussed in Section 4.1 and the corresponding w_i is scaled down by the same factor; these operations have effects on the weighted sums of energy functions because the energy values within each frame of discernment are scaled while those outside the frames remain at value -1. Although MRF #2 is more intuitive as the log scale gives zero energy to the correct label in an ideal scenario, it performs worse than MRF #1 and MRF #1+.
- The last three rows are classifiers that apply Gaussian naive Bayes on the 46 features from the NBR classifier. There are two choices of features: Gaussian naive Bayes #1 and #1+ use $\text{sigmoid}(s_i \cdot G_i(\text{image}))$, $i \in \{1, \dots, 46\}$, as features, while Gaussian naive Bayes #2 uses $G_i(\text{image})$. The difference between Gaussian naive Bayes #1 and #1+ is that a step is added in #1+ that mimics Dempster-style scaling: the feature values are scaled up as discussed in Section 4.1; note that there is no corresponding operation to the scaling of b_i ’s in an NBR classifier or the scaling of w_i ’s in MRF #1+.

Among the seven ablation-study models, MRF #1+ is

the clear winner. In fact, it can be viewed as a poor man’s NBR classifier: it contains the same L2NNNs and a step that mimics Dempster-style scaling, yet it replaces the top-level belief-function operations with weighted sums. The effect is that it reduces computational complexity at the cost of accuracy and robustness.